APPLIED AND ENVIRONMENTAL MICROBIOLOGY, Feb. 1985, p. 434–440
0099-2240/85/020434-07$02.00/0

Vol. 49, No. 2

Kinetic Studies of Bacterial Sulfate Reduction in Freshwater Sediments by High-Pressure Liquid Chromatography and Microdistillation

KEES A. HORDIJK, CHARLES P. M. M. HAGENAARS, AND THOMAS E. CAPPENBERG*
Limnological Institute, Vijverhoflaboratory, 3631 AC Nieuwersluis, The Netherlands

Received 31 October 1984/Accepted 8 November 1984

Indirect photometric chromatography and microdistillation enabled a simultaneous measurement of sulfate depletion and sulfide production in the top 3 cm of freshwater sediments to be made. The simultaneous measurement of sulfate depletion and sulfide production rates provided added insight into microbial sulfur metabolism. The lower sulfate reduction rates, as derived from the production of acid-volatile $^{35}S^{2-}$ only, were explained by a conversion of this pool to an undistillable fraction under acidic conditions during incubation. A mathematical model was applied to calculate sulfate reduction from sulfate gradients at the sediment-water interface. To avoid disturbance of these gradients, the sample volume was reduced to 0.2 g (wet weight) of sediment. Sulfate diffusion coefficients in the model were determined ($D_s = 0.3 \times 10^{-5}$ cm^2 s^{-1} at 6°C). The results of the model were compared with those of radioactive sulfate turnover experiments by assessing the actual turnover rate constants (2 to 5 day^{-1}) and pool sizes of sulfate at different sediment depths.

An understanding of the coupling between sediments and the overlying water requires a knowledge of the mechanisms controlling both nutrient remineralization rates and chemical exchange across the sediment-water interface. The respiratory reduction of sulfate to sulfide is one of the dominating processes in the metabolism and diagenesis of anoxic sediments, although the quantitative importance of detrital breakdown by sulfate-reducing organisms is just beginning to be appreciated. Studies on brackish sediment in Denmark (12, 21) have shown the importance of bacterial sulfate reduction in the annual mineralization of organic matter in marine sediments. Sulfate reduction in freshwater sediments may also be very significant (4, 10, 18–20) if, despite low concentrations of free sulfate, large pools of alkyl-sulfate esters are produced photosynthetically in the water layer and an internal sediment-surface recycling process is operative. Recent data obtained in our laboratory (2a) suggest that sulfate reduction as a terminal process in anaerobic carbon mineralization plays a more important role in freshwater sediments than was previously understood. In the mesotrophic stratifying Lake Vechten, The Netherlands, 8 to 20% of the amount of sedimented particulate organic carbon is converted to CO_2-carbon by sulfate reduction. The lake is described in detail elsewhere (22).

As a result of analytical difficulties in determining the pool sizes of sulfate in interstitial water in freshwater sediments, data on the quantification of sulfate reduction by existing ^{35}S radiotracer methods (13) or mathematical modeling (1) are essentially lacking for low-sulfate environments. Recently, we have developed a method to determine sulfate in freshwater-sediment interfaces by indirect photometric chromatography (IPC), which gives well-defined sulfate profiles in the micromolar range for the sediments in Lake Vechten (7). In this method, separation is achieved by competition between the strongly UV-absorbing anion and the solute anions for the ion-exchange sites on the column. It follows that elution of sulfate will be accompanied by a localized deficiency of the UV-absorbing anions in the eluent. The presence of the anion in the solute is then shown by a drop in the base-line value, which is proportional to the amount injected.

In this paper we describe the dynamics of sulfate reduction with the use of a mathematical model involving vertical sulfate gradients as a function of diffusion, bacterial reduction, and sedimentation. The rates of sulfate reduction and sulfide production were also determined directly in sediment cores by a $^{35}SO_4^{2-}$ radiotracer technique that involves the use of microdistillation, which is assumed not to disturb the most active superficial sediment layer during sampling by minimizing the total amount of mud needed for analyses. Special attention was paid to the calculation of the turnover rates by assessing the actual turnover rate constants (k values) and actual pool sizes of sulfate at different sediment depths; this was done by determining the in situ concentration profiles and the depletion of $^{35}SO_4^{2-}$ by IPC. Finally, the rates were compared with those calculated from the model as a means of understanding the kinetics of bacterial sulfate reduction and internal sediment sulfate recycling.

MATERIALS AND METHODS

Sulfate analysis. The liquid chromatograph consisted of a model 1330 Bio-Rad pump with a model 1305 Bio-Rad UV detector (Bio-Rad Laboratories, Richmond, Calif.). Samples were introduced by using a Rheodyne 7125 valve with a 20-μl loop, which was replaced by a 200-μl loop for the radioactivity measurements. The column (75 by 4.6 mm; HPLC Technology, Cheshire, England) was packed with 5-μm Nucleosil SB anion exchange particles. A guard column (75 by 2.1 mm, type B for anion exchange chromatography; Chrompack, Middelburg, The Netherlands) was used. The columns were insulated with cotton batting for temperature stability. An eluent of 5-sulfoisophthalic acid buffer (0.4 mM, monosodium salt diluted in distilled water [pH 4.5]; Aldrich, Beerse, Belgium) was used. Detection was at 239 nm with a flow rate of 0.8 ml/min; the attenuation was 0.16 absorbance units at full scale with the 200-μl loop. Concentrations were evaluated by external standardization. For calibration, a series of gravimetric standard solutions in the range of 0 to

* Corresponding author.

250 μM (0 to 25 μg/ml) sulfate were made in double-distilled water. Calibration curves were made by plotting the peak heights obtained from the chromatograms of the standards against the original standard solutions. The peak heights obtained from the sample chromatograms were compared mathematically with those of the standards for analysis. The molar response factors used were obtained from the calibration curves. More details on eluent effects, reduction of retention time, and recovery of the sulfate fractions from the sediments are given in a description of an earlier version of the method (7).

Sample collection. Samples were collected with the exclusion of oxygen to prevent possible oxidation of reduced sulfur to sulfate. A modified Jenkin surface mud sampler was used to collect undisturbed mud cores from the deepest part of the eastern depression of Lake Vechten (2). For the measurement of sulfate concentration profiles, subsamples of 0.2 to 1.5 g, depending on the water content of the sediments, were horizontally drawn by piercing the syringe through the 2-mm holes (covered with Scotch tape no. 471) in the acrylic glass sampling tube. The upper water layer was removed to prevent mixing of the sulfate-rich water layer with the sulfate-poor sediment water. The subsamples were transferred into mini-vials (Pierce Chemical Co., Rockford, Ill.) with different volumes (maximum volume, 1.5 ml) and short, conical bottoms. The vials were completely filled with sediment and immediately closed with screw-capped Teflon-faced disks and centrifuged for 5 to 10 min at 1,000 × *g* at room temperature. After centrifugation, the supernatant was immediately separated from the sediment and stored at −20°C on analysis. After thawing, organic Fe(III) complexes were formed. The Fe(III) cations originated from the excess of free $Fe^{II}CO_3$ (23) dissolved in the pore water of Lake Vechten. The formed iron coprecipitates were removed by a second centrifugation, and 20 μl of the supernatant was injected into the high-pressure liquid chromatograph for sulfate analysis. Injection of unfreezed supernatant showed that the freezing procedure had no measurable influence on the sulfate concentration in the supernatant, as all the reduced sulfur was precipitated in the first centrifugation step.

Model of SO_4^{2-} dynamics. Berner (1) described a theoretical model to estimate the rate of sulfate reduction from measured sulfate profiles by the equation

$$\left.\frac{\partial C}{\partial t}\right|_x = D_s \frac{\partial^2 C}{\partial x^2} - \omega \frac{\partial C}{\partial x} - f(x)$$

In this formula C is the measured sulfate concentration at time t, D_s is the diffusion coefficient, ω is the rate of sedimentation, and $f(x) = a \cdot e^{-bx}$, a function describing first-order sulfate reduction. When the system is in steady state, a practical solution of $f(x)$ in this diffential equation is given by:

$$\int_{x_1}^{x_2} f(x)dx = -(C_o - C_\infty)(\omega + D_s b)e^{(x_2 - x_1)}$$

where C_o is the sulfate concentration of the overlying water layer, C_∞ is the minimum sulfate concentration, and b could be computed by fitting the function $C_x = (C_o - C_\infty) \cdot e^{-bx} + C_\infty$ on the measured sulfate profile.

Diffusion measurements. The application of the model requires an independent determination of the diffusion constant D_s. One method of estimating D_s is the instantaneous source technique (5). Here the diffusion profile developed from a momentary release from a thin layer placed above the sediment is used. Measurements for the instantaneous source technique were done in a subcore (12 by 3 cm) at the environmental temperature of 6°C. To suppress sulfate reduction, the sediment was mixed with Na_2MoO_4 at a final concentration of 20 mM, which is 100 times higher than the concentration necessary for complete inhibition of sulfate-reducing activity in freshwater sediments (20). The subcore was incubated overnight at 6°C; on the following day a 0.5-cm layer of water containing 10 mM Na_2SO_4 was carefully placed above the sediment, and the core was incubated for 3.75 h before the sulfate concentration profiles were measured. The diffusion coefficient is found from the equation

$$\log_{10} C_{(x,t)} = a(t) - \frac{x^2}{4 D_s t} \cdot \log_{10} e$$

where $C_{(x,t)}$, the concentration at depth x, is obtained from the sulfate concentration profile at time t and $a(t)$ is a function of time. For a constant t, $a(t)$ is constant and D_s can be calculated from the slope of the regression line of a plot of x^2 against $C_{(x)}$.

A second method of estimating D_s is the constant source technique (5). Here the diffusion profile developed from a constant sulfate input is used. The measurements were done in an intact Jenkin core with a water layer containing 20 mM Na_2MoO_4 35 cm above the sediment. After 24 h, the permeation of MoO_4^{2-} suppressed sulfate reduction in the sediment. At this time sulfate was added to the upper water layer to a final concentration of 10 mM. The column was incubated overnight. On the following day the sulfate concentration profile in the upper 4 cm of the sediment was measured. The diffusion constant D_s is then determined from the equation

$$C_{(x,t)} = C_o \cdot \text{erfc}\,[x/2(D_s t)^{1/2}]$$

where at time t the concentration C_x at depth x is obtained from the sulfate concentration profile. C_o is constant in time, and erfc denotes the complementary error function. D_s was estimated from the error function graph described by Duursma and Hoede (5).

$^{32}SO_4^{2-}$ batch experiments. For estimating sulfate reduction rates, sediment samples (20 ml) were taken anaerobically at different depths from a Jenkin core by syringe and transferred into 30-ml serum vessels. The serum vessels were capped with butyl rubber stoppers, and the headspace was flushed with oxygen-free nitrogen. The sediment batches were mixed with Na_2SO_4 (final concentration, 2 mM) and placed into an Perspex jar (GasPak; BBL Microbiology Systems, Cockeysville, Md.) for anaerobic incubation for 14 days at 4°C with gentle mixing. During incubation, subsamples of the sediment were taken and analyzed for sulfate.

$^{35}SO_4^{2-}$ tracer experiments. Undiluted sediment samples (6 ml) from various depths were taken horizontally from the Jenkin core, as described above, for incubation with $Na_2{}^{35}SO_4$. The samples were anaerobically transferred into 7-ml pico-vials (Packard, Brussels, Belgium). Each pico-vial was capped with a butyl rubber stopper, and the headspace (1 ml) was flushed for 5 min with oxygen-free nitrogen which had passed through a column of BASF catalyser R3-11 at 150°C. After the headspace had been flushed, an anaerobic solution containing 1.78×10^5 dpm of $Na_2{}^{35}SO_4$ in 0.1 ml of distilled water (Amersham Corp., Little Chalfont, England) was added by piercing the rubber stopper with a syringe. The sediment samples in the pico-vials were stirred vigorously on a Vortex mixer for a uniform distribution of the

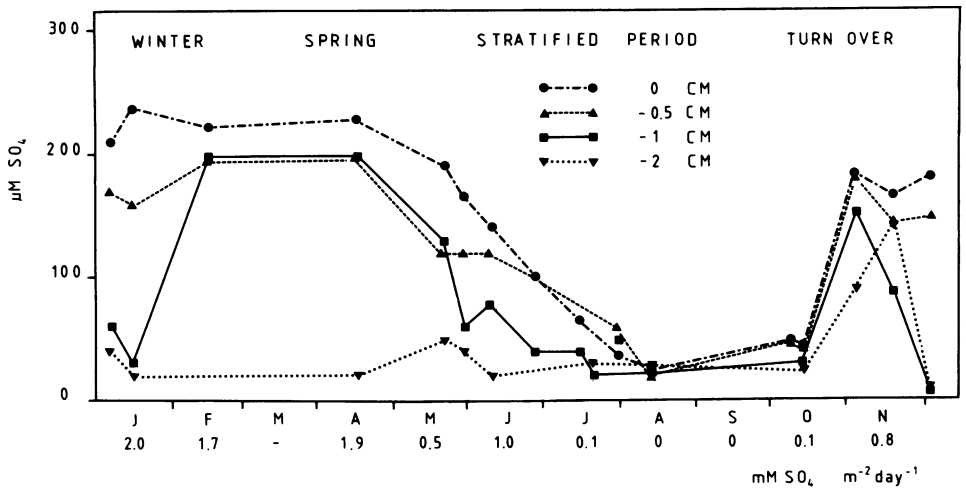

FIG. 1. Sulfate concentrations in the pore water of the upper 2 cm of sediment in Lake Vechten in 1983. The sulfate reduction rates obtained from the profiles and calculated from the model are given for each month. The horizontal axis has two scales; the upper scale shows time in months and the lower scale shows sulfate reduction rates in millimoles of SO_4^{2-} per square meter per day.

$^{35}SO_4^{2-}$ label. The samples were incubated in the dark at 6°C (in situ temperature). During the incubation, 1-ml samples were taken with a syringe at hourly intervals. No change in the natural pH (7.2) was observed. The samples were transferred into pico-vials which were previously flushed with nitrogen.

The pico-vials were immediately weighted and centrifuged at 1,000 × *g* for 1 min at room temperature. After centrifugation, 300 µl of pore water was withdrawn by syringe, transferred into centrifuge tubes, and stored at −20°C for sulfate analysis. The centrifuged pico-vials with the precipitated sediment were frozen by immersion in an acetone-dry ice mixture for 15 min and stored under nitrogen for subsequent distillation and radiochemical analysis. For simultaneous $^{35}SO_4^{2-}$ and $^{32}SO_4^{2-}$ measurements, the frozen pore water was thawed and centrifuged before injection into the high-pressure liquid chromatograph. The $^{32}SO_4^{2-}$ concentration was measured by the UV detector as described above. For $^{35}SO_4^{2-}$ measurements, a 6-ml fraction which included the sulfate peak volume (3 ml) was collected in a scintillation vial to which 11 ml of Instagel II (Packard) was added. The radioactivity in the vials was counted in a Packard Tri Carb 4530 liquid scintillation spectrometer for 20 min at a window breadth of 4-167 KeV. Quench curves of the eluent (0.4 mM 5-sulfoisophthalic acid) showed an excellent count efficiency (95% or more), in contrast to that of the untreated pore water (below 60%). This efficiency is explained by the complete separation of the sulfate peak from potential quenching components (organics and cations) and the lack of absorbance of the eluent above 300 nm, in which spectrum region the scintillator emits. Calibration curves with a calculated amount of radioactivity (1,000 to 1,500 dpm per 200-µl injection) that were used for external standardization and for correction of the decay time (87.9 days) were linear (r = 1.00000). Standard addition of $^{35}SO_4^{2-}$ to the sediment showed a recovery of 98.5% from the pore water.

The $^{35}S^{2-}$ produced from the same sediment samples were measured by a modification of the method of Jørgensen (13) on the day of incubation. The modification was the substitution of a microdistillation apparatus which consisted of the pico-vial containing the frozen sediment sample after centrifugation and two pico-vial traps in series connected by a short segment of thick-wall Teflon tubing. Seven units were placed parallel on a Perspex glass plate for simultaneous distillation. The traps contained 2 ml of zinc acetate solution, 0.5 ml of NaOH, and 0.1 ml of isoamyl alcohol. It proved essential to add the isoamyl alcohol as antifoam in the microdistillation apparatus. The samples were stirred with microbars and tape-recorder motors which were mounted under a Perspex glass plate. Before distillation, the system was flushed with oxygen-free nitrogen. At this stage the samples were still frozen. The nitrogen flow (± 5 ml min^{-1}) was adjusted for each sample unit to prevent cross-contamination by siphoning. Distillation of the acid-volatile sulfide was initiated by the addition of 1 ml of 4 N HCl, which reduced the pH of the sediment to 0. The liberated $H_2{}^{35}S$ was carried with the nitrogen into the pico-vial traps within 40 min. A solution of 5 ml of Instagel II (Packard) and 0.1 ml of NaOH was added to the traps for measurement with the scintillation counter. Standard addition experiments in which a series of $Zn^{35}S$ (382 to 1,520 dpm) was added to the sediment showed a linear recovery of 89 ± 7% (r, 0.9981) of the liberated $H_2{}^{35}S$ in the first trap. Quench curves of $Zn^{35}S$ made in the trap mixture showed an efficiency of 95%. We used ZnS to see whether the added amount of HCl was sufficient to release the volatile metal-bound sulfide pool and whether the released $H_2{}^{35}S$ was quantitatively trapped in the distillation train. The results agree with those found by Ingvorsen et al. (10).

Sulfate reduction rates were calculated from the formula

$$\text{rate} = k \cdot [^{32}SO_4^{2-}] = \frac{\ln(N_o/N)}{t} \cdot [^{32}SO_4^{2-}]$$

where N_o is the added $^{35}SO_4^{2-}$ (disintegrations per minute per cubic centimeter), N is the $^{35}SO_4^{2-}$ rest activity at time t (days), and $[^{32}SO_4^{2-}]$ is the sulfate concentration obtained from the sulfate profile in the sediment (nanomoles per cubic centimeter).

Sulfide production rates calculated from the formula (13)

$$\text{rate} = \frac{[^{32}SO_4^{2-}] \cdot (^{35}S^{2-})}{(^{35}SO_4^{2-}) \cdot t}$$

where $[^{32}SO_4^{2-}]$ is the sulfate concentration (nanomoles per

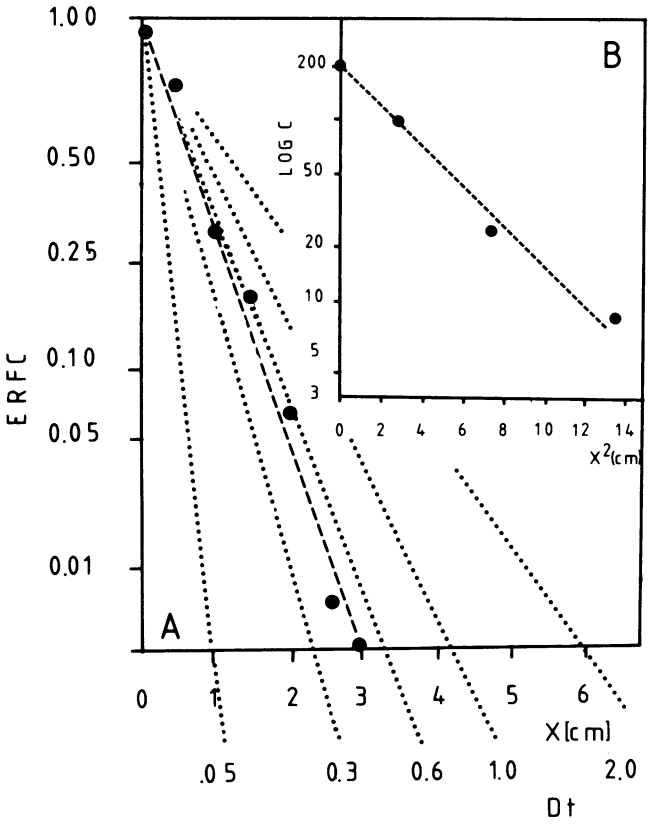

FIG. 2. (A) Plot of the inward diffusion of sulfate (stripes) from the water column into the sediment of a Jenkin core (constant source model). The scale on the vertical (y) axes of the graph was calculated from the complementary error function (ERFC) to arrive at a linear relation between the depth x (cm) and the fraction C_x/C_o (y coordinate). The diffusion coefficient D_s can be estimated from $D_s \times t$ by interpolation between lines (dotted) drawn for different Dt values (5). (B) Plot of the inward diffusion of sulfate from a momentary release from a thin (0.5-cm) water layer into a sediment subcore by using the instant source model. C (concentration of SO_4^{2-}) is plotted on a vertical logarithmic scale to arrive at a linear relation with the square of the depth (centimeters), from which slope D_s can be calculated.

cubic centimeter) of the sediment, ($^{35}SO_4^{2-}$) and ($^{35}S^{2-}$) are the sulfate and sulfide radioactivities (disintegrations per minute), and t is the incubation time (days).

RESULTS

Sulfate concentrations in the top 2 cm of the sediment decrease at the beginning of the summer stratification (Fig. 1). In the summer and early autumn the sulfate concentrations are low, and early in October the sulfate concentrations increase again. The deeper layers (1 and 2 cm deep) showed a second fall in sulfate concentration in the autumn and early winter. This is not observed in the more superficial layers of the water column just over the sediment. With the vertical sulfate profiles at the sediment-water interface, sulfate-reducing activities (Fig. 1) were estimated by the diffusion model. In the model, the diffusion constant calculated from the constant source ($[0.3 \pm 0.05] \times 10^{-5}$ cm^2 s^{-1}) (Fig. 2A) and from the instant source ($[0.3 \pm 0.03] \times 10^{-5}$ cm^2 s^{-1}) (Fig. 2B) were used. These values are similar to those for marine sediments if corrected for temperature (16, 17). The sedimentation rate (1.8×10^{-3} cm day^{-1}) was estimated from the thickness of the organic layer in the lake (20 to 30 cm) and the time in which this layer was deposited, namely about 40 years (22). The sulfate reduction rates obtained from the model (Fig. 1) at the 1-cm-deep layer roughly parallel the sulfate concentration. The highest sulfate reduction rates (2 mM m^{-2} day^{-1}) were observed in winter, whereas during summer stratification in August and September no sulfate reduction in the sediment was found.

A second estimation of sulfate-reducing activity was derived from the decrease in sulfate in a stagnant water column over a sediment core (Fig. 3). During the first 13 days of the incubation at 4°C, sulfate gradients were developed in the water phase, and from these profiles, a sulfate reduction of 0.6 mM m^{-2} day^{-1} was estimated. When the water column was mixed by gentle air bubbling, release of sulfate (5 mM m^{-2} day^{-1}) from the sediment occurred.

A third estimate of the sulfate-reducing activity was derived by following sulfate depletion in $^{32}SO_4^{2-}$-enriched sediment samples (10 times the natural concentration). During the first 7 days, sulfate reduction rates were linear, the highest being 107 to 110 nmol cm^{-3} day^{-1} in the batches from the upper 2 cm of the sediment, followed by 22 to 30 nmol cm^{-3} day^{-1} in batches from 2 to 6 cm and 6 nmol cm^{-3} day^{-1} in batches from 6 to 10 cm. After 7 days, the sulfate reduction rates in the batches increased, resulting in complete depletion of the sulfate pool in the batches from the upper few centimeters within 14 days. The total sulfate reduction from the sediment surface (1.7 mmol m^{-2} day^{-1}) was calculated by summation of the areal sulfate reduction rates.

The fourth estimate of sulfate-reducing activity is derived from the conversion of $^{35}SO_4^{2-}$ to $^{35}S^{2-}$. A logarithmic decrease of $^{35}SO_4^{2-}$ with time at various depths was observed for at least 3 h (Fig. 4A). Using the turnover rate constants derived from Fig. 4A (Table 1) and the actual in situ pool sizes which remained constant during incubation,

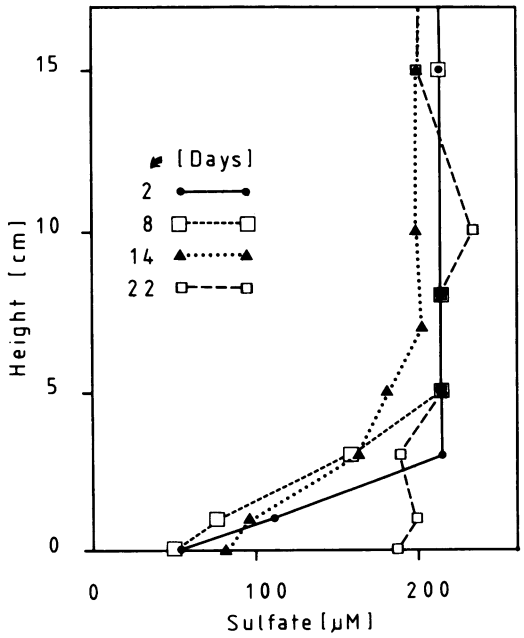

FIG. 3. Sulfate profiles in a stagnant water column above the sediment of a Jenkin core measured at different time intervals during the 22-day incubation at 4°C.

we calculated sulfate reduction rates for different depths at the sediment-water interface (Table 1). The summed sulfate-reducing activity for the different depths was 3.6 mM m^{-2} day^{-1}. A logarithmic increase of acid-volatile $^{35}S^{2-}$ was simultaneously observed in the same samples (Fig. 4B). the $^{35}S^{2-}$ generated in this experiment represents a significant proportion (33% or more) of the $^{35}SO_4^{2-}$ added to the sediment. The efficiency of conversion appears to increase with depth (Table 1). Summation of the turnover rates of $^{35}SO_4^{2-}$ obtained from the production rate constants of $^{35}S^{2-}$ (Table 1) gives a total sulfate reduction rate of 1.6 mM m^{-2} day^{-1}.

To determine the variation in sampling, sediment batches were taken from five different Jenkin cores at a depth of 2 cm. The batches were incubated at in situ temperature, and the conversion of $^{35}SO_4^{2-}$ into $^{35}S^{2-}$ was followed until the added $^{35}SO_4^{2-}$ (±21,000 dpm cm^{-3}) was nearly depleted (Fig. 5). A maximum of 80% of the added $^{35}SO_4^{2-}$ was recovered in the acid-volatile $^{35}S^{2-}$ pool after 1 h. The sulfate reduction rate in these samples was much faster than those shown in Fig. 4. The $^{35}S^{2-}$ in the sediment generated from the reduction of $^{35}SO_4^{2-}$ showed a loss with time after nearly all the $^{35}SO_4^{2-}$ had been depleted. The same phenomenon was observed in the inhibition experiments with 20 mM Na_2MoO_4 (Fig. 5). The addition of 20 mM Na_2MoO_4 completely inhibited the depletion of $^{35}SO_4^{2-}$ in the sediment

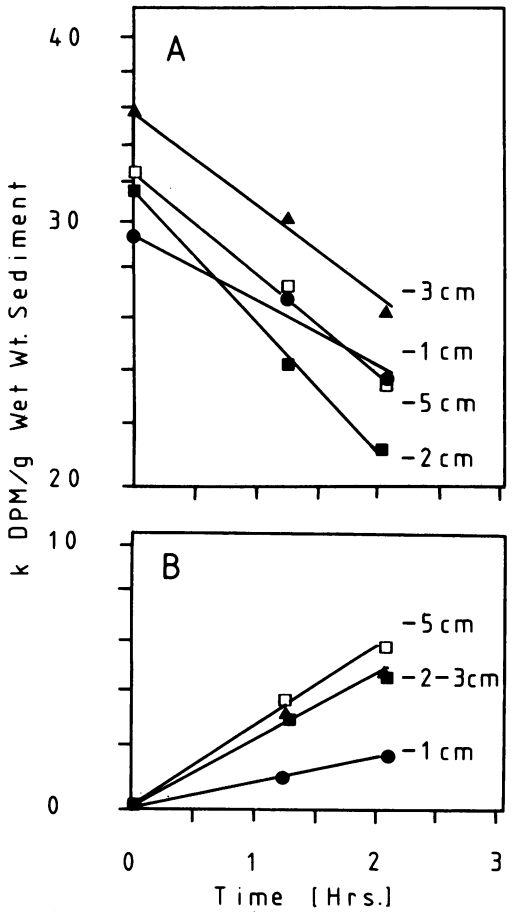

FIG. 4. Depletion of $^{35}SO_4^{2-}$ (A) and the production of $^{35}S^{2-}$ (B) on semi-log scale in sediment batches from several depths in the upper 5 cm of a Jenkin core.

TABLE 1. Sulfate depletion and sulfide production in sediment batches from Lake Vechten, calculated from the data in Fig. 4

Sample depth (cm)	Pool size of sulfate (μM)	Turnover rate constant (day^{-1})	Sulfate reduction (nmol cm^{-3} day^{-1})	Sulfide production (nmol cm^{-3} day^{-1})	Recovery (%)[a]	Recovery (%)[b]
1 ± 0.2	86 ± 10	2.1 ± 0.5	185 ± 65	61 ± 7	33	98
2 ± 0.2	32 ± 5	3.2 ± 0.4	107 ± 23	70 ± 22	65	108
3 ± 0.2	12 ± 5	3.2 ± 0.4	41 ± 20	24 ± 10	59	104
5 ± 0.2	3 ± 1	5.1 ± 0.4	24 ± 5	9 ± 3	38	101

[a] Percentage of sulfate recovered in the sulfide fraction.
[b] Recovery of $^{35}SO_4^{2-}$ at time t_0 after 1 min of mixing.

batches after 0.5 h, after which the acid-volatile $^{35}S^{2-}$ pool decreased logarithmically and the $^{35}SO_4^{2-}$ remained constant.

DISCUSSION

The dynamics of sulfate reduction in sediments were generally investigated by following the sulfide production (8, 10, 14, 15, 18–20), since a sensitive (microliter) method for determining sulfate was not available. With the recent introduction of liquid chromatography in sedimental sulfate analysis (7), it is now possible to measure sulfate depletion directly rather than analyze one of its conversion products (S^{2-}). Also, for accurate measurement of the easily disturbed steep gradients of sulfate (Fig. 1), only small samples (0.2 g [wet weight]) as used by IPC prevented mixing of the sediment layers. IPC is preferred for studying the conversion processes of sulfate in freshwater, since the technique is

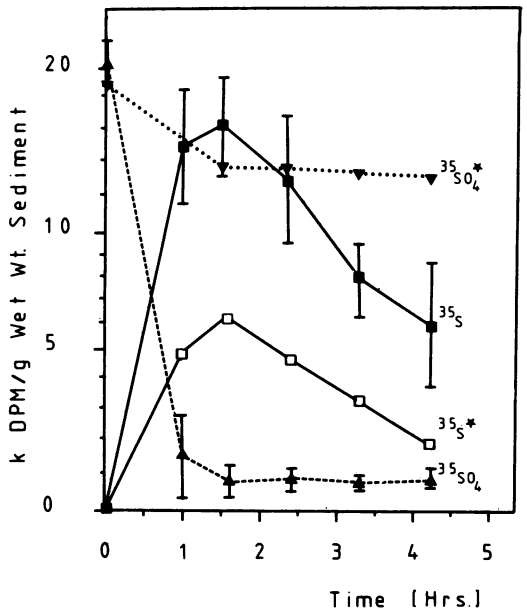

FIG. 5. Average depletion of acid-volatile ^{35}S in anaerobically incubated sediment batches of samples (from a depth of 2 cm) in five different Jenkin cores. The acid-volatile ^{35}S was generated by the conversion of $^{35}SO_4^{2-}$. (*) Inhibition effect of Na_2MoO_4 addition (after 1 h of incubation) on the conversion of $^{35}SO_4^{2-}$ into acid-volatile ^{35}S. Note the depletion of ^{35}S while the $^{35}SO_4^{2-}$ concentration remains constant.

TABLE 2. Comparison of sulfate reduction rates obtained from the model and from batch experiments

Method	Sulfate reduction rate (mM m^{-2} day^{-1})
Diffusion model	1.8
Incubation of stagnant cores	0.6
Batch incubation with $^{35}SO_4^{2-}$	1.7
Batch incubation with $^{35}SO_4^{2-}$	
Depletion of $^{35}SO_4^{2-}$	3.6
Production of $^{35}S^{2-}$	1.6

neither laborious nor difficult to set up. Since the sediments are not exposed to air, the risk of oxidation artifacts is considerably reduced. The reduction rates obtained from the model are mainly determined by the steepness of the measured concave-down profile, which were normally not found in marine sediments (14), since mixing within the core will smooth the natural gradient, resulting in an underestimation of the sulfate-reducing activity.

In Lake Vechten, sulfate-reducing activities were correlated with the seasonal fluctuation of the sulfate concentration in the lower layers of the lake (23). During summer stratification the sulfate in the hypolimnion is supplied mainly through diffusion from the metalimnion. In this period, sulfate reduction is low in the sediment and occurs in the hypolimnion. This is also evident from the sulfate depletion in the hypolimnion and the presence of sulfate-reducing bacteria in this layer (2). The relation between carbon input and sulfate consumption in the deepest water stratum and in the sediments of Lake Vechten was studied with the help of diffusion flux calculations and sedimentation measurements. At the start of the summer stratification, about 19% of the input carbon was mineralized by sulfate reduction, but at the end of the summer stratification this was about 8% (22a).

During the autumnal overturn, both increased turbulence and oxygen supply to the lower water layers result in a net production of sulfate that reappeared in the overlying water of the sediment. In winter, when the water layers in the lake are remixed, an equilibrium between sulfate conversion processes is established so that the concentration of sulfate in the lake does not change. The turbulence effect was imitated by the aerobic incubation of intact Jenkin cores (Fig. 3), which showed that the amount of sulfate withdrawn from the overlying water is controlled by the turbulence of the water layer. Oxygen and redox potential measurements by microelectrode techniques in the sediments of intact Jenkin cores showed a rapid decrease of 10 μg/ml to 0.5 μg of O_2 per ml and a redox potential fall of 170 mV in the upper 4 mm of the sediment, excluding chemical reoxidation of the reduced sulfur below this layer. These observations confirms the results of the model which showed the highest sulfate-reducing activity in the same small layer (0.5 to 2.5 cm deep) of the maximum abundance of sulfate-reducing bacteria (2).

Anaerobic incubation of sulfate-enriched sediment batches from this layer with sulfate concentrations 10 times the natural ones showed that the sediment can reduce this excess of sulfate completely without the limitation of the organic pool. This was indicated previously by assessing the pool sizes and turnover rates of important lower fatty acids (3, 6). The absence of the organic limitation permits first-order kinetics in the model, and no sulfate adsorption to the sediment was found (7). Sulfate reduction in the anaerobic sediment of Lake Vechten is therefore limited by the available sulfate concentration supplied by diffusion.

Comparison of the results of the model (Table 2) with those from the batch experiments in the same sulfate-reducing zone (0 to 5 cm deep) showed that reducing rates observed by incubation with $^{35}SO_4^{2-}$ (Fig. 4 and 5) were higher. This may be explained by the direct availability of sulfate from recycling processes to the sulfate-reducing bacteria in the upper 5 mm of the sediment. These recycling processes are not measured by the diffusion model. The applied model gives an estimate of the net sulfate reduction rates and may be useful in routine studies for comparing sulfate-reducing activities in different freshwater sediments.

The most reliable sulfate reduction rates in sediments are obtained by measuring the depletion rate of sulfate simultaneously with their pool size; this gives the actual turnover rates. From the acid-volatile sulfide depletion shown in Fig. 5, it may be concluded that sulfate reduction rates in freshwater sediments are easily underestimated if only sulfide production is followed. This is because the addition of molybdate (Fig. 5) shows that when sulfate reduction is completely inhibited, the formed sulfide slowly depletes. The lower sulfate reduction rates derived from the production of acid-volatile $^{35}S^{2-}$ can be explained by a slow conversion of this pool to an undistillable fraction. The acid distillation does not include $^{35}S^{2-}$ label incorporated into compounds as pyrite and elemental sulfur, which must be determined by other means (9). It was recently reported (8, 9, 11, 15) that only 30% of the converted $^{35}SO_4^{2-}$ ends up in the acid-volatile pool which is recovered by distillation. In Lake Vechten sediment, 50% of the acid-volatile pool is converted into the non-acid-volatile pool within 3 h (Fig. 5). Howarth and Merkel (9) reported the rapid formation of pyrite in salt marsh sediments. From Fig. 5 we can conclude that after 1.5 h more than 85% of the reduced sulfur was present as $Fe^{35}S$. For this reason, we believed as a result of sequential reactions the reduced ^{35}S is more likely to end up in inorganic (FeS_2,S_0) instead of organic compounds. The incomplete recovery of all the reduced sulfur compounds by the acid distillation complicates an accurate estimation of sulfate-reducing activity in the sediment. For this reason, IPC is an additional, nearly indispensable, tool for studying the conversion processes of sulfate in freshwater.

ACKNOWLEDGMENTS

We thank David C. White (Florida State University, Tallahassee) and our colleagues Henk Verdouw and Ramesh D. Gulati for helpful manuscript reviews. We also thank H. L. Lindeboom (Delta Institute for Hydrobiological Research, Yerseke, The Netherlands) for microelectrode measurements, H. Roon for assistance in the field, E. M. Mariën for photography, and M. C. G. Röling for typing the manuscript.

LITERATURE CITED

1. **Berner, R. A.** 1964. An idealized model of dissolved sulfate distribution in recent sediments. Geochim. Cosmochim. Acta **28**:1497–1503.
2. **Cappenberg, T. E.** 1974. Interrelations between sulfate-reducing and methane-producing bacteria in bottom deposits of a freshwater lake. I. Field observations. Antonie van Leeuwenhoek J. Microbiol. Serol. **40**:285–295.
2a. **Cappenberg, T. E., C. A. Hordijk, and C. P. M. M. Hagenaars.** 1984. A comparison of bacterial sulfate reduction and methanogenesis in the anaerobic sediments of a stratified lake ecosystem. Arch. Hydrobiol. Beih. Ergebn. Limnol. **19**:191–199.
3. **Cappenberg, T. E., and E. Jongejan.** 1978. Microenvironments for sulfate reduction and methane production in fresh-water

sediments, p. 129–138. *In* W. E. Krumbein (ed.), Environmental biochemistry and geobiology, vol. 1. Ann Arbor Science Publishers, Ann Arbor, Mich.

4. **Cappenberg, T. E., and H. Verdouw.** 1982. Sedimentation and breakdown kinetics of organic matter in the anaerobic zone of Lake Vechten. Hydrobiologia **95**:165–179.
5. **Duursma, E. K., and C. Hoede.** 1967. Theoretical, experimental and field studies concerning molecular diffusion of radioisotopes in sediments and suspended solid particles of the sea. Neth. J. Sea Res. **3**:423–457.
6. **Hordijk, C. A., and T. E. Cappenberg.** 1983. Quantitative high-pressure liquid chromatography-fluorescence determination of some important lower fatty acids in lake sediments. Appl. Environ. Microbiol. **46**:361–369.
7. **Hordijk, C. A., C. P. M. M. Hagenaars, and T. E. Cappenberg.** 1984. Analysis of sulfate at the mud-water interface of freshwater lake sediments using indirect photometric chromatography. J. Microbiol. Methods **2**:49–56.
8. **Howarth, R.** 1979. Pyrite: its rapid formation in a salt marsh and its importance in ecosystem metabolism. Science **203**:49–51.
9. **Howarth, R., and S. Merkel,** 1984. Pyrite formation and the measurement of sulfate reduction in salt marsh sediments. Limnol. Oceanogr. **29**:598–608.
10. **Ingvorsen, K., J. G. Zeikus, and T. D. Brock,** 1981. Dynamics of bacterial sulfate reduction in a eutrophic lake. Appl. Environ. Microbiol. **42**:1029–1036.
11. **Jones, J. G., B. M. Simon, and J. V. Roscoe.** 1982. Microbiological sources of sulfide in freshwater lake sediments. J. Gen. Microbiol. **128**:2833–2839.
12. **Jørgensen, B. B.** 1977. The sulfur cycle of a coastal marine sediment (Limfjorden, Denmark). Limnol. Oceanogr. **22**:814–832.
13. **Jørgensen, B. B.** 1978. A comparison of methods for the quantification of bacterial sulfate reduction in coastal marine sediments. 1. Measurement with radiotracer techniques. J. Geomicrobiol. **1**:11–27.
14. **Jørgensen, B. B.** 1978. A comparison of methods for the quantification of bacterial sulfate reduction in coastal marine sediments. 2. Calculations from mathematical models. J. Geomicrobiol. **1**:29–47.
15. **King, G. M.** 1983. Sulfate reduction in Georgia salt marsh soils: an evaluation of pyrite formation by use of ^{35}S and ^{55}Fe tracers. Limnol. Oceanogr. **28**:987–995.
16. **Lerman, A.** 1979. Diffusion coefficients in solution, p. 79–100. *In* A. Lerman (ed.), Geochemical processes water and sediment environments. John Wiley & Sons, Inc., New York.
17. **Li, Y. H., and S. Gregory.** 1974. Diffusion of ions in sea water and deep-sea sediments. Geochim. Cosmochim. Acta **38**: 703–714.
18. **Lovley, D. R., and M. J. Klug.** 1983. Sulfate reducers can outcompete methanogens at freshwater sulfate concentrations. Appl. Environ. Microbiol. **45**:187–192.
19. **Smith, R. L., and M. J. Klug.** 1981. Reduction of sulfur compounds in the sediments of a eutrophic lake basin. Appl. Environ. Microbiol. **41**:1230–1237.
20. **Smith, R. L., and M. J. Klug.** 1981. Electron donors utilized by sulfate-reducing bacteria in eutrophic lake sediments. Appl. Environ. Microbiol. **42**:116–121.
21. **Sørensen, J., B. B. Jørgensen, and N. P. Revsbeck.** 1979. A comparison of oxygen, nitrate, and sulfate respiration in coastal marine sediments. Microb. Ecol. **5**:105–115.
22. **Steenbergen, C. L. M., and H. Verdouw.** 1982. Lake Vechten: aspects of its morphometry, climate, hydrology and physicochemical characteristics. Hydrobiologia **95**:11–23.

22a. **Steenbergen, C. L. M., and H. Verdouw.** 1984. Carbon mineralization in microaerobic and anaerobic strata of Lake Vechten (The Netherlands): diffusion flux calculations and sedimentation measurements. Arch. Hydrobiol. Beih. Ergebn. Limnol. **19**:183–190.

23. **Verdouw, H., and E. M. J. Dekkers.** 1980. Iron and manganese in Lake Vechten (The Netherlands); dynamics and role in the cycle of reducing power. Arch. Hydrobiol. **89**:509–532.